European network
for developing new horizons for RIs

## Project information

| | |
|---|---|
| **Project full title** | European network for developing new horizons for RIs |
| **Project acronym** | EURIZON |
| **Grant agreement no.** | 871072 |
| **Instrument** | Research and Innovation Action (RIA) |
| **Duration** | 01/02/2020 – 31/01/2024 |
| **Website** | https://www.eurizon-project.eu/ |

## Deliverable information

| | |
|---|---|
| **Deliverable no.** | 5.9 |
| **Deliverable title** | Final report on R&D work on particle identification system for the SCT detector |
| **Deliverable responsible** | JLU |
| **Related Work-Package/Task** | *Work package 5:* Lepton Colliders<br>Joint technology development around future lepton colliders / *Task 5.6:* Development and design of a Particle Identification system |
| **Type (e.g. Report; other)** | Report |
| **Author(s)** | Simon Bodenschatz, Michael Düren, Jens Sören Lange (corresponding author), Mustafa Schmidt, Marc Strickert, Jhonatan Pereira de Lira |
| **Dissemination level** | Public |
| **Document Version** | |
| **Date** | |
| **Download page** | |

## Document information

| Version no. | Date | Author(s) | Comment |
|---|---|---|---|
| 1.0 | 31.10.2023 | Lange | For review in group. |
| 2.0 | 03.11.2023 | Lange | For review in group and alumni. |
| 2.1 | 08.11.2023 | Schmidt | Corrections, additional figures. |
| 2.2 | 08.11.2023 | Düren | Corrections. |
| 3.0 | 09.11.2023 | Lange | Figure numbering fixed, conclusion added. |
| | | | |
| | | | |
| | | | |
| | | | |

This project has received funding from the European Union's Horizon 2020 research and innovation programme under grant agreement No. 871072.

## [Table of Contents]



# Program EU HORIZON 2020, Nr. 871072

**Final Report**

***Work package 5:*** **Lepton Colliders**
**Joint technology development around future lepton colliders**

***Task 5.6:*** **Development and design of a Particle Identification system for a future flavour factory detector**

***Deliverable 5.9***

## 1. Particle identification requirements for future experiments

Searches for new physics in e+e- collisions are demanding higher energies or higher luminosities. The Super Tau Charm Factory (STCF) is designed to provide luminosities up to $10^{35}$ $cm^{-2}$ $s^{-1}$ at center-of-mass energies of 2-6 GeV, which is more than one order of magnitude larger compared to the existing BESIII experiment at the BEPC II accelerator. Such high luminosities would enable searches for rare lepton-flavor violating decays such as $\tau \rightarrow \mu\gamma$.

For a detector at the STCF, this would imply a stringent particle identification requirement of a $3\sigma$ $\mu/\pi$ separation from 0.5 up to 1.2 GeV/c particle momentum. So far, this has not been achieved by experiments. For a corresponding momentum range, the reported separation at BaBar was about $2.4\sigma$, at Belle between 2.5 and $2.8\sigma$, and at KEDR about $2.9\sigma$.

This project has received funding from the European Union's Horizon 2020 research and innovation programme under grant agreement No. 871072.

For a Cherenkov detector providing the particle identification, this separation translates into a required resolution of the Cherenkov angle of 1 mrad (0.7 mrad) resolution at 1.2 (1.5) GeV/c. The μ/π separation in the given momentum range for the instrumentation of a DIRC detector using materials with high refractive indices as shown in Fig. 1.

For different parts of the physics program (e.g. D meson decays), a π/K-separation more than 4σ up to 2.5 GeV/c is required. As technically this would correspond to a μ/π separation at 6 GeV/c, this requirement is already within the boundaries described above. This separation has been achieved by experiments, e.g. the DIRC barrel detector at the BaBar experiment with about 4σ up to 2.5 GeV/c, but to our knowledge only in barrel-type detectors and not in endcap detectors.

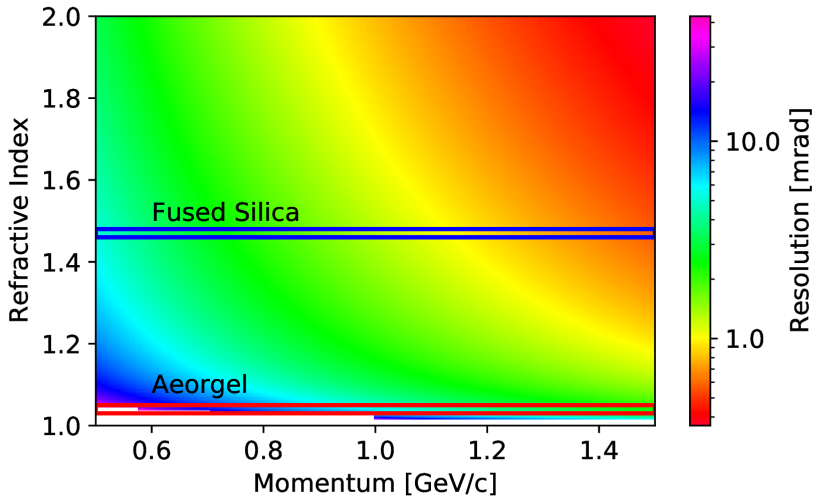


*Fig 1: Required detector resolution for μ/π separation as a function of the particle momentum and refractive index*

One of the main difficulties to reach that resolution in the Cherenkov angle, is dispersion in both the radiator and the materials of the optical system. Thus, as described below, a precise dispersion correction must be pursued. In addition, as a requirement, the e+e- collisions would imply a symmetric forward/backward detector design. Different from fixed target experiments such as e.g. PANDA, an endcap Cherenkov detector would cover a wider polar angular range, with consequences for the design of the optical focusing system. Another issue is related to induced systematic errors due to the angle straggling of the primary particle in densed materials like fused silica. This issue, however, has to be addressed separately and is not part of the detector development itself.

On a technical level, there are requirements in the environment of the detector operation which have to be addressed. The expected high luminosities also imply high background levels, and therefore radiation hardness of frontend readout components becomes an issue. Additionally, issues of the operation of the photon sensors in a high magnetic field of 1 Tesla and under cooling temperatures of down to T=–40°C are addressed in this report.

This project has received funding from the European Union's Horizon 2020 research and innovation programme under grant agreement No. 871072.

This report is the second part of the presentation of the particle identification R&D within the EURIZON project. We refer to [Sch21] for the basic introduction and documentation of preliminary results.

## 2. Prototype Cherenkov detector setups

### 2.1 Giessen Cosmic Station (Readout with MCP-PMTs)

The Giessen Cosmic Station (GCS, see Fig. 2) is the prototype of the disk-shaped disc DIRC (Detection of Internally Reflected Cherenkov light) detector. The structure is the size of a quadrant (i.e. 25% of a disc, see Fig. 3, right), designed for a total of 24 ReadOut Modules (ROM, see Fig. 4) and 7200 readout channels. In the prototype tests reported hereafter, two ROMs were connected. The GCS detects muons from cosmic radiation with a minimum momentum of 600 MeV/c, by using 45 cm thick lead plates. The detection surface of the GCS is comparable in size to the endcap detectors in the STCF design with about 0.6912 $m^2$. The setup reached a position resolution of 0.5 cm and an angular resolution of 3.5 mrad. For details, we refer to [Bod20].

In the starting phase, the GCS data acquisition was implemented as free streaming and triggerless, corresponding to the mode that is envisaged e.g. for the PANDA experiment. Precise synchronization and data matching based upon timestamps was utilized to reconstruct full events. In a later stage, within the EURIZON project, in 2021 trigger counters were installed [Wel21] above and below the Cherenkov detectors, each of them with 4 photon detectors at the edges. Designs with Si-PMs (Silicon photomultipliers, efficiency measured up to 73%) and conventional PMTs (photomultiplier tubes, efficiency measured up to 78%) were installed, which required inverting the signal polarity in the latter case. The trigger counters enabled coincidence logic operations.

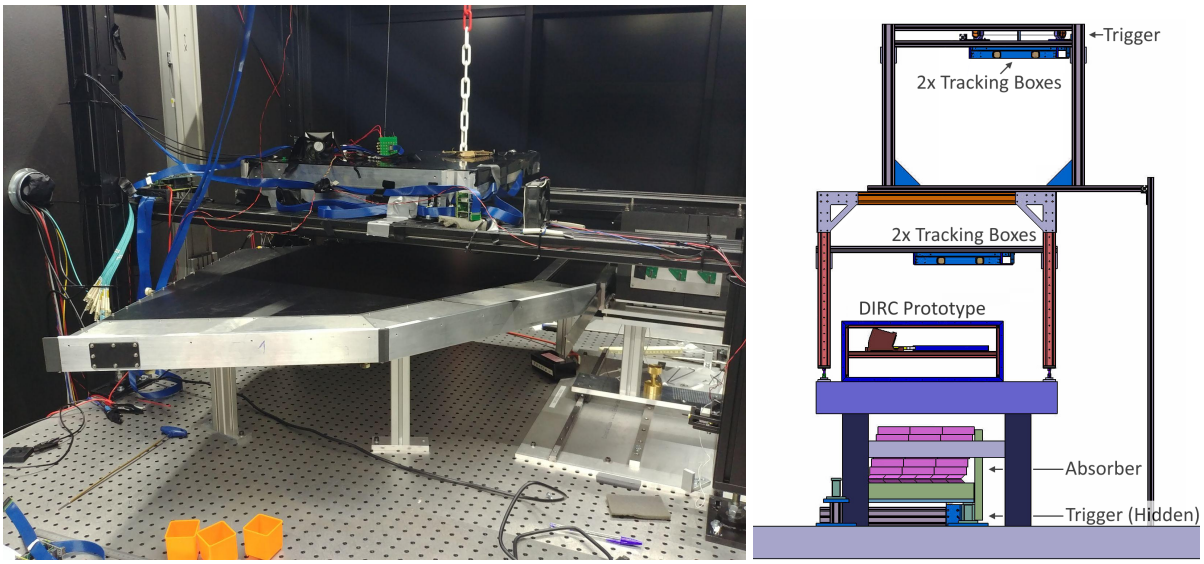


*Fig. 2: Photo (left) and schematic setup of the Giessen Cosmic Station (GCS).*

This project has received funding from the European Union's Horizon 2020 research and innovation programme under grant agreement No. 871072.

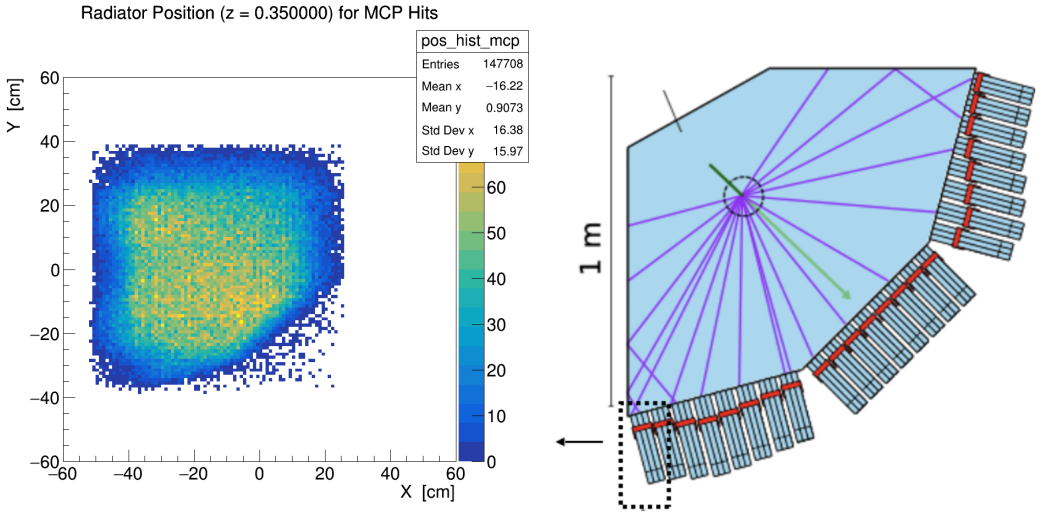


*Fig. 3: Radiator of the GCS. Left: Position of MCP hits inside the radiator. Right: Schematic top view. The dashed box comprises one ROM.*

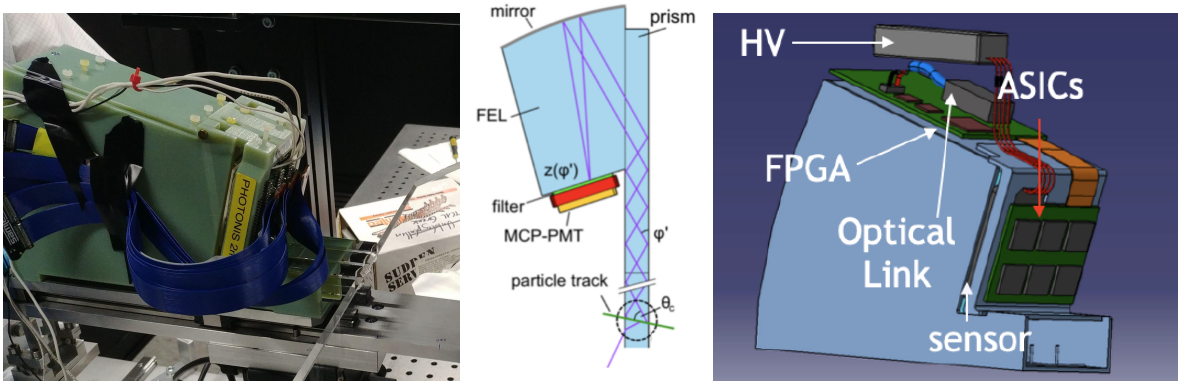


*Fig. 4: Photo of a ROM (left), path of Cherenkov photons inside a ROM (center) and schematic side view of a ROM (ReadOut Module) of the GCS.*

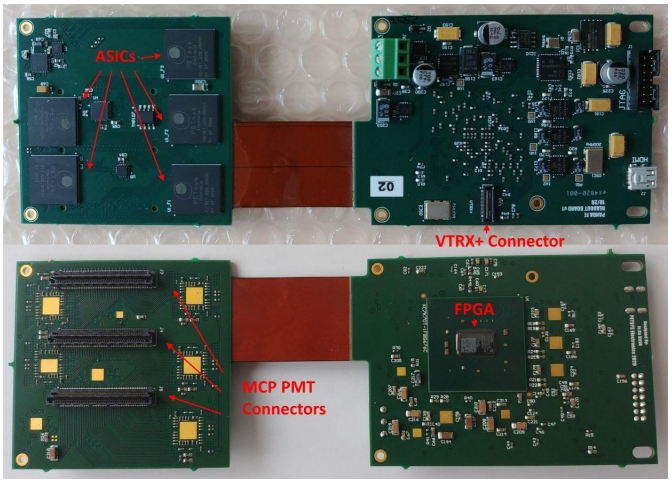


*Fig. 5: Custom PCB (Printed Circuit Board) for the readout at the GCS.*

This project has received funding from the European Union's Horizon 2020 research and innovation programme under grant agreement No. 871072.

Several work packages regarding mechanics and electronics were finished within the EURIZON project [Kös21]. Examples are the 3D construction of the optical light path, the change from air cooling to liquid cooling, and the design and fabrication of a custom readout PCB (printed circuit board), shown in Fig. 5. The board uses five TOFPET ASICs (Fig. 5, left) and one Kintex Ultrascale FPGA (Fig. 5, right). Data are streamed out to the backend via VTRX+ connectors. The PCB has advanced features such as AC coupling, native handling of negative signal polarity, radiation hard optical links, and DC–DC converters without large inductance [Kös21].

Within the EURIZON project, the GCS setup was optimized in two ways, on the one hand by adding more pixel rows to the MCP-PMTs and on the other hand by precise positioning and alignment [Brü22]. Furthermore, long-term operation and data taking was performed over 4+ months [Brü22].

### 2.2 Mini Giessen Cosmic Station (Readout with Si-PMs)

The Mini-GCS is a smaller detector physically built on top of the GCS, which was integrated into the DAQ of the GCS and therefore can be read out in coincidence. Matrices of KETEK Silicon Photomultipliers (Si-PMs, type PA3325-WB-0808) and Hamamatsu Si-PMs (type S13361-3050AE-08) SiPM's are used, respectively, each with 8x8 pixels of 3x3 mm² size. Above the sensors, support structures for radiators are mounted. Cosmic muons can generate rings of Cherenkov light, which can be detected with the SiPM's. Magnesium fluoride and quartz glass were tested as radiator materials; the photon yield on the sensors is between 10 and 13.

In the Mini-GCS, the sensors are mounted with a polar angle of $13^{o}$ concerning the radiator. Therefore, Cherenkov rings appear as curves in the projection. A fit of the curves in combination with the knowledge of the polar angle of the primary muons can be used to determine the Cherenkov angle [Hof22].

### 2.3 CERN test beam experiments

A prototype detector with a radiator of 500 × 500 $mm^2$ and 20 mm thickness was tested in the Proton Synchrotron (PS) test area T9 beam in August 2018 at CERN. The prototype consisted of 5 ROMs, each with 3 optical light focussing elements and one MCP-PMT, with 128 x 6 channels (Hamamatsu, type YH0245) or 100 x 3 channels (Photonis, types XP85132-S-MD3 and XP85132-Q-MD3-HA). The goal was to measure the PID performance with a momentum scan from 7 GeV/c to 10 GeV/c for a mixed π/p beam. The polar angle is from 4 to 22 degrees, covering about 50% of the polar angle coverage at STCF. The results were compared to Monte-Carlo simulations. Additional test beam experiments could not be performed due to the worldwide pandemic situation.

## 3. Cherenkov angle resolution

### 3.1 Geometry of Cherenkov angle reconstruction

Fig. 6 shows schematically the Cherenkov light propagation and assigns all required angular variables. The Cherenkov angle $\theta_c$ can be reconstructed using the following formula:

$$\theta_c = \arccos(\sin\theta_p \cos\varphi_{rel} \cos\phi + \cos\theta_p \sin\phi)$$

This project has received funding from the European Union's Horizon 2020 research and innovation programme under grant agreement No. 871072.

Here $\theta_p$ is the angle of incidence of the primary particle impinging onto the radiator, and it needs to be known e.g. by tracking detectors. $\phi$ denotes the angle between the photon path and the radiator surface. The angle $\varphi_{rel}$ is defined as the angle between the measured photon and the trajectory of the primary particle, while $\phi'$ is the angle measured by the sensor. The following relation provides the required geometrical transformation:

$$\tan \phi' = \tan \phi / \cos \alpha_{FEL} \ ,$$

where $\alpha_{FEL}$ is the angle between the active FEL and the photon trajectory.

In [Sch17], the Cherenkov angle reconstruction algorithm was implemented on a XILINX Virtex FPGA. The resolution was found to depend on the bit precision of the representation of integer numbers within the FPGA firmware. For 16-bit precision, a Cherenkov angle resolution of about 2 mrad was achieved [Sch17].

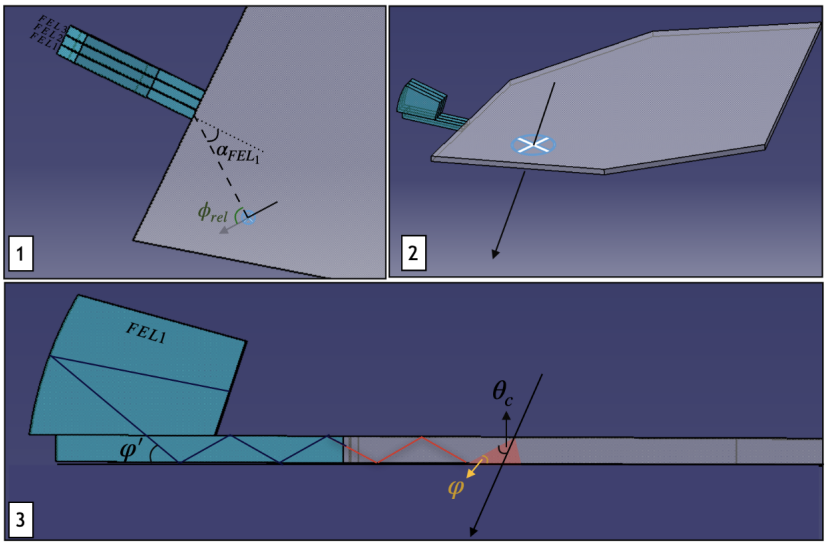


*Fig 6: Geometry definitions for the reconstruction of the Cherenkov angle. [1] Top view of the radiator with three focussing elements (FEL). The angle between the charged particle and the FEL is $\alpha_{FEL}$. [2]: The isometric view of the radiator with the position of the charged particle traversed. [3]: The side view of the setup with a Cherenkov light cone (red) and the angles.*

### 3.2 Results of Cherenkov angle resolution

The Pattern of channel number vs. reconstructed position, which is often referred to as the "Cherenkov smile" pattern and is shown in Fig. 7.

Although the CERN test beam experiment was performed in 2018, the data were analyzed within the EURIZON project. In particular, the separation of protons and pions could be investigated here, since these two particle species were in the beam. For high beam momenta of 5-10 GeV/c Cherenkov angles of 0.817 rad for protons and 0.825 rad for pions were measured, with a resolution determined as 5-11 mrad [Kös21] (see Fig. 8). The pion/proton separation power was determined as 3σ at 7 GeV/c momentum, with a relative misidentification of about 2%.

This project has received funding from the European Union's Horizon 2020 research and innovation programme under grant agreement No. 871072.

In the GCS, the Cherenkov angle for muons with a momentum of higher than 600 MeV/c was determined as about 0.8 rad with a resolution determined as 12 mrad [Kös21] (see Fig. 9).

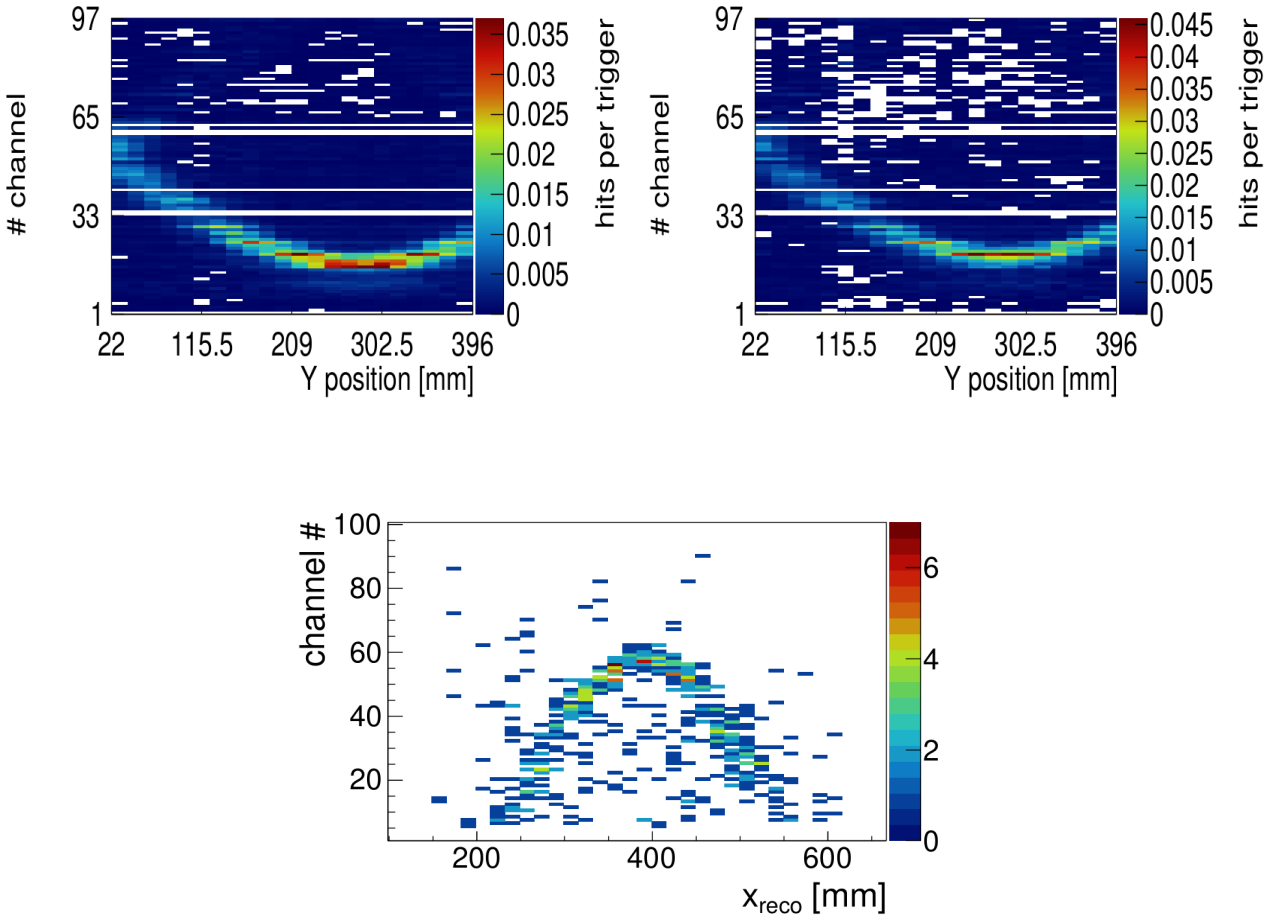


*Fig. 7: Pattern of channel number vs. reconstructed position, which is often referred to as "smile" pattern, for the GCS (top) and the CERN test beam experiment (pions, bottom left and protons, bottom right). Due to the specific geometries, the pattern can be mirrored, as seen here in the GCS.*

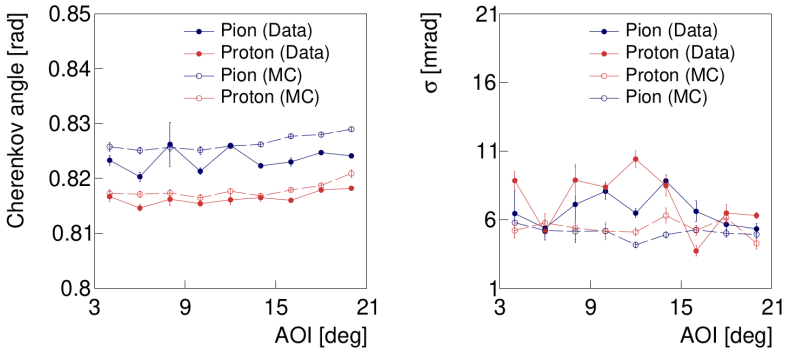


*Fig 8: Cherenkov angle (left) and single photon resolution (right) for different angle of incidence (AOI) of the beam with respect to the radiator in the CERN testbeam experiment at 7 GeV/c.*

This project has received funding from the European Union's Horizon 2020 research and innovation programme under grant agreement No. 871072.

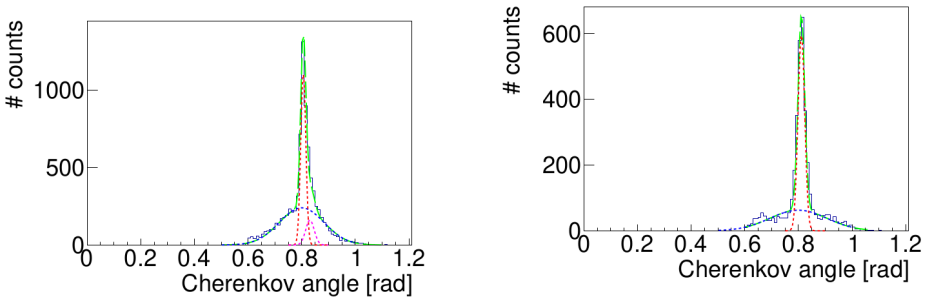


*Fig. 9: Reconstructed Cherenkov angle for cosmic muons in the GCS (left: data, right: MC). The fitted width represents the Cherenkov angle resolution.*

### 3.3 Single Photon Detection

Cherenkov angle resolutions for single photon events are useful as a figure-of-merit for comparison between detectors in different experiments. As a rule of thumb, the final resolution improves with ~1/√N, with N representing the number of detected Cherenkov photons. In a testbeam experiment at DESY, a single photon resolution of 7.4 mrad was measured [Sch17], which can be scaled for a final resolution of 2.5 mrad with N=14. For an improved quantitative estimate, additionally outlier removal, the detector topology (i.e. square or circular shape of the radiator, and the tracking resolution for the determination of the angle-of-incidence should be taken into account, which gives 1.5 mrad [Sch17].

In a high statistics measurement of 4 4-month duration in the GCS, the Cherenkov angle resolution was determined separately for one-photon as 6.49-9.04 mrad [Brü22]. The predicted difference of resolutions from the MC is smaller than the experimental errors (14.8%) and therefore cannot be confirmed, yet. As a side result of the measurement, the two-photon time resolution was determined to be 386–655 ps [Brü22]. The variation arose from different readout modules using either Hamamatsu or Photonis MCP-PMTs.

A pulsed UV laser with a wavelength of 403 nm was used [Tak21] in order to study the possible detection of single Cherenkov photons with KETEK Si-PMs (type PM3350-EB). By variation of the diameter of the laser spot, the frequency, and the light yield using an attenuator, asymptotically it can be reached that single photons impinge on the Si-PMs. At room temperature, the dark count rate was very high at 4.5 MHz and led to misleading signals. Cooling with dry $C0_2$ ice was tried, keeping the temperature in the setup to about T=–70°C and reducing the dark rate to about 40 kHz. Using the cooled setup, single photon and multiple photon signals could be distinguished clearly in the amplitude spectra. However, as a technical disadvantage, the cooling led to condensation and ice formation on the Si-PM electronics.

Comparing Hamamatsu and KETEK Si-PM Arrays, the different applied voltages must be taken into account: 57.6 V for Hamamatsu and 31.5 V for KETEK. Overvoltage can be applied in both systems; an overvoltage of 3 V leads to the following numbers: S/N for Hamamatsu around 4.58, S/N for KETEK around 1.83, and ratio of signals for Hamamatsu and KETEK around 3.25.

This project has received funding from the European Union's Horizon 2020 research and innovation programme under grant agreement No. 871072.

### 3.4 Dispersion correction

The problem of dispersion and dispersion correction was investigated within the design of the geometry of the optical system to be built e.g. for application at the STCF. Detailed simulations of the paths of the individual photons were performed [Keg22]. The optical focusing elements (FEL) consist of lenses, mirrors, and prisms. In the following, the angle of incidence (AOI) is the angle between the normal of the radiator surface and the particle. One of the most important figure-of-merit parameters is the root mean square of the photon position distribution („rms“). Dispersion plays a role in two effects:

1.) Dispersion in the radiator leads to smearing of the Cherenkov angle. In general, the Abbe number is a measure of the strength of a material's dispersion Fused silica as the radiator material of choice has a relatively high Abbe number of 67.8, while higher Abbe numbers correspond to lower dispersion.

2.) Dispersion in the optical path behind the radiator (e.g. in the glass of the lens) is subject to chromatic aberration, i.e. wavelength-dependent refractive index of the lens material which causes photons of different wavelengths to be refracted to different degrees. The Cherenkov angle of 0.829 rad for 300 nm drops to 0.807 rad at 800 nm. This wavelength range is one of the requirements for future accelerators. In particular, the lower boundary of 300 nm is a consequence of using the radiation hard glue Epotek-2 to connect the optical elements, which is only transparent above this limit. By shrinking the wavelength range, the detector resolution can additionally be enhanced as shown in Fig. 10. This can be achieved either on one hand by inserting a wavelength filter or on the other hand by selecting a photosensor with a quantum efficiency range in the desired spectrum. It turned out that Photonis provides high-QE photocathodes in the orange to red spectrum which would improve the detector performance significantly. However, these materials have a much shorter lifetime and radiation-induced degradation compared to photocathodes in the blue-to-green spectrum.

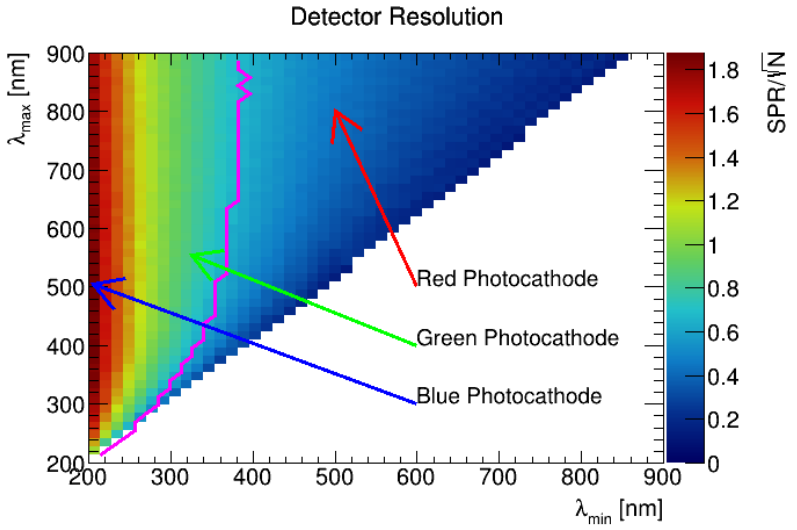


*Fig. 10: Calculated detector resolution for all possible wavelength ranges in the visible spectrum.*

This project has received funding from the European Union's Horizon 2020 research and innovation programme under grant agreement No. 871072.

The solution of a wavelength filter, as being discussed for the PANDA experiment, however comes with the disadvantage of removing Cherenkov photons. As mentioned above, the number of Cherenkov photons N improves the Cherenkov angle resolution according to a $1/\sqrt{N}$ scaling factor. As this resolution is one of the most important requirements for the STCF, the primary objective in the EURIZON project was to investigate different, possibly more challenging technical solutions. In the design of the optical system, there can be two ways to apply dispersion correction:

As a first step, the right choice of materials it is in some cases possible to partially reduce the effects of the dispersion by utilizing an additional optical component with an additional dispersion added to the focusing optics. An example is the insertion of a LiF prism between the radiator and an optical element behind in the optical path (e.g. a mirror or a lens). However, this is not straightforward as there are difficulties with LiF. Although the material is technically radiation-hard, the creation of color centers after irradiation is possible, which causes the formation of several absorption bands between 300 and 500 nm.

In [Wet22] a simulation of two complete DISC DIRC detectors was performed, with LiF prism (i.e. design for the STCF) and without a LiF prism (i.e. design for the PANDA experiment). The prism is inserted in the optical path for dispersion correction by counteracting the effects of dispersion smearing the Cherenkov angle of the emitted photons. The design with the prism is often referred to as „sandwich design“. The separation power for kaons and pions was studied, however, for the sandwidth design, contrary to prior expectation, found to be smaller over the complete range of polar angles and momenta. The reason is given by the different required kinematical ranges, i.e. polar angles from 10° to 40° with lower momenta from 0.2 GeV/c up to 1.5 GeV/c for STCF, compared to smaller polar angles from 5° to 22° and higher momenta from 1.0 GeV/c and 4.0 GeV/c at PANDA. The much larger angular region coverage makes it much harder to find an optimum focusing geometry. At this point, it cannot even be excluded that such a geometry may not even be existing.

In a second step, for additional dispersion correction in a lens-based system, the simplest setup would be a lens doublet with two different glasses. Assuming that the radiator is made of fused silica, for the first lens one would use a radiation-hard glass with a high refractive index compared to fused silica, for example N-LAK. For the dispersion correction, then N-LAK and N-SF6 or N-LAK and K5G20 could be combinations. A way of visualization of the effect of the dispersion correction is shown in Fig. 9. For or a combination of two materials, the ratio of the two refractive indices should be as flat as possible as a function of wavelength. For 100% dispersion correction the curve would be a flat and constant line. One combination namely LAK9G15 and F2G12 is especially interesting because the wavelength-dependent ratio of the refractive indices is one of the few in Fig. 11 which show a positive slope.

This project has received funding from the European Union's Horizon 2020 research and innovation programme under grant agreement No. 871072.

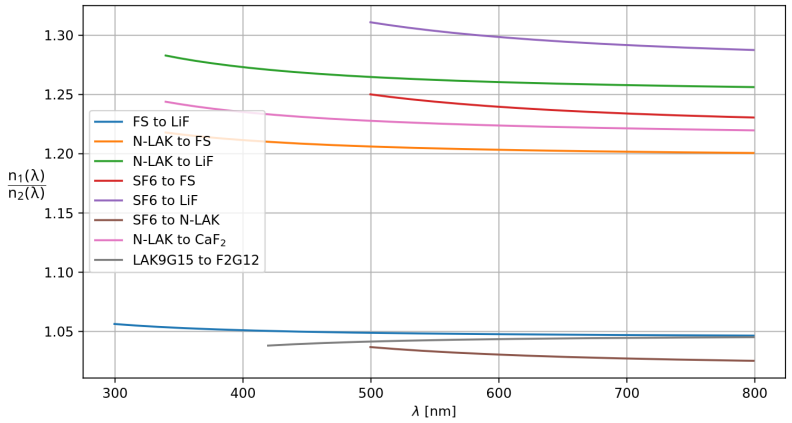


*Fig. 11: Visualization of the effect of dispersion correction in a combination of two materials, in particular here two radiation hard types of glasses with high refractive indices.*

There are two possible main directions for the design of the optical system: mirror-based or lens-based.

In a mirror-based focusing system the focusing does not depend on the wavelength of the photon but on its angle. Several mirror-based designs were studied [Keg22], but as an important result, for all mirror-based FEL the rms shows large values of 1.3 mm or more at high values of the angle of incidence . This is at least a factor 4 worse then for lens-based systems, as will be shown below. This makes the use of a mirror-based system very limited at an STCF, and even impossible at angles of incident beyond 35° instead of the intended 40°.

Thus, as a main result of our studies, lens-based systems should be preferred and were also studied in detail [Keg22].

One of the main questions is, if single or multiple lenses should be used. From a performance point of view, systems with two lenses (rms determined as 0.4-0.7 mm) are about a factor 3 better than a system with one lens only (rms determined as 1.0-1.1 mm). However, a single lens provides a lower detectable wavelength of 340 nm, while the best two-lens system has a lower cutoff of 500 nm and is therefore unacceptable.

As mentioned above, a different question is the choice of MCP-PMT, as different types provide different quantum efficiencies (QE) for different wavelengths. In particular, MCP-PMTs with a red-light-sensitive cathode, with high QE for wavelengths 400-500 nm, and a green-light-sensitive cathode, with high QE for wavelengths 500-850 nm have been compared. The result is not straightforward, because an efficiency correction for the sensor must be applied. For angles below 20 degrees, red cathode is better (rms 0.7 vs rms 0.8 mm), and for angles above green cathode type is better (rms 0.8 mm vs. rms ≥0.9 mm)

Fresnel lenses with a complex design have been studied as well. They have originally been developed for lighthouses and can be thought of as one lens divided into several sections, with a surface of

This project has received funding from the European Union's Horizon 2020 research and innovation programme under grant agreement No. 871072.

edges and regions of different curvature. Fresnel lenses can be thinner by a factor ≥2 compared to conventional lenses, however, our result is that for the Cherenkov application, their rms is comparable in the order of 0.3-0.4 mm.

# 4 Environment of detector operation

## 4.1 Radiation hardness

In addition to the glasses in the optical system (see above), also the readout PCBs are installed close to the radiator and their components may be subject to radiation effects. Using a strong $^{60}$Co source, electronic components were exposed up to doses of 4870 Gray [Pap23]. This is much more than expected at STCF and even more than expected over the lifetime of PANDA with about 10 Gray. The results are as follows:

1.) All resistors are radiation hard; no variation of the resistances was observed.

2.) All capacitors lost about 10% of their inductance, but were still operating.

3.) Among the tested voltage regulators, NCP59748 and NCP59744 are radiation hard and should be preferred for future experiments. LT3020EDD stopped functioning after 801 Gray; no output voltage was measured thereafter. While on the other hand TPS76833 was still functioning after 801 Gray, problems were observed after 3344 Gray; an output voltage could still be measured, but unregulated and linearly rising with the input.

## 4.2 Influence of cooling

The Cherenkov single photon detection requires effective cooling in order to keep the dark count rate at a minimum. It was observed that interestingly a variation of the cooling temperature from T=–40°C to T=–20°C has a significantly different impact on different types of Si-PMs in the Mini GCS setup. While for Hamamatsu Si-PMs the dark count rate rises by only 10% from about 100 kHz to about 110 kHz, for KETEK Si-PMs it rises by a factor of 3 from about 100 kHz to about 300 kHz [Bod24].

## 4.3 Influence of magnetic field

As a test, the PCB with the ASICs and the FPGA (see Fig. 5) has been operated in a magnetic field of 1.000±0.015 Tesla. A pulser generating signals with similar picosecond pulse shape characteristics as signals from an MCP-PMT was used. No negative effect was observed.

# 5. Applications of Machine Learning

Cosmic muons have not only a polar angle, but also an azimuthal angle when they enter the GCS. The Reconstruction of the azimuthal angle of the cosmic muons in the Mini-GCS was attempted. As described above, in the Mini-GCS Cherenkov rings are observed as curves. In addition, the curves are asymmetric due to their projection to a non-zero azimuthal angle of the primary muon. In [Hof22] it was tried to reconstruct the azimuthal angle with a 4-layer neural network, using the hit pattern of the 128 pixels as input. A resolution of about 12 degrees was achieved.

This project has received funding from the European Union's Horizon 2020 research and innovation programme under grant agreement No. 871072.

One TOFPET ASIC has 64 input channels from one readout module. Input signals of neighboring readout modules on the radiator [Pap23] are related in a non-trivial way. Due to the same origin of the primary Cherenkov light, the firing pattern of the 64 signals of one ASIC is a high-dimensional function of the firing pattern of the 64 signals of the other ASIC. A multilayer perceptron was trained to represent this function. The figure-of-merit of the correct prediction of the input of the neighboring ASIC is the mean absolute error (MAE). An MAE of 1.0 corresponds to 64 wrongly predicted channels. An MAE of 0.5 corresponds to a random prediction (i.e. 32 wrongly predicted channels). The quantitative result is an MAE of 0.226 (corresponding to 14.5 wrongly predicted channels). This demonstrates that in case of malfunction of one ASIC, the missing data of this ASIC can be predicted with an accuracy of about 49.5 correctly predicted signals among a total of 64.

In [Per23] an improvement of the reconstruction of the Cherenkov angle by use of Neural Networks (NN) was attempted, by using additional information of A total of 600 parameters are input into the NN. 300 input nodes received the on/off status of the MCP-PMT detectors. As additional information, 200 input nodes received the on/off status of the GCS tracking detectors in the respective event, which encodes the particle direction. Additional 100 input nodes received the number of Cherenkov photons in the range 0.6 rad to 1.0 rad. Two NN architectures were used, namely a Multilayer Perceptron (MLP) and a Convolutional Neural Network (CNN). The result is that by using the NN, the resolution of the Cherenkov angle is improved by more than a factor of 2, from 35-36 mrad (RMS) up to 15-16 mrad (RMS). The quantitative improvement is approximately the same for both MLP and CNN.

## 6. Outreach

At the EURIZON detector school in Wuppertal, Germany, July 17-28, 2023, the Giessen group provided four hands-on tutorials. In an MCP-PMT tutorial, a delay line anode was used (see Fig. 12, left), in which the time of propagation along the surface of the anode can be measured. Based on the arrival times and their differences it is possible to reconstruct the location of the charge cloud. The spatio-temporal sensor resolution was determined by fitting with the CERN root package. A second tutorial covered the assembly and readout of a do-it-yourself electron spectrometer using low-cost components (see Fig. 12, right). The goals of the experiment were gaining soldering practice, and understanding signal amplification circuits. Two additional tutorials covered the detection of cosmic muons and the implementation of an STCF prototype detector in Geant4.

This project has received funding from the European Union's Horizon 2020 research and innovation programme under grant agreement No. 871072.

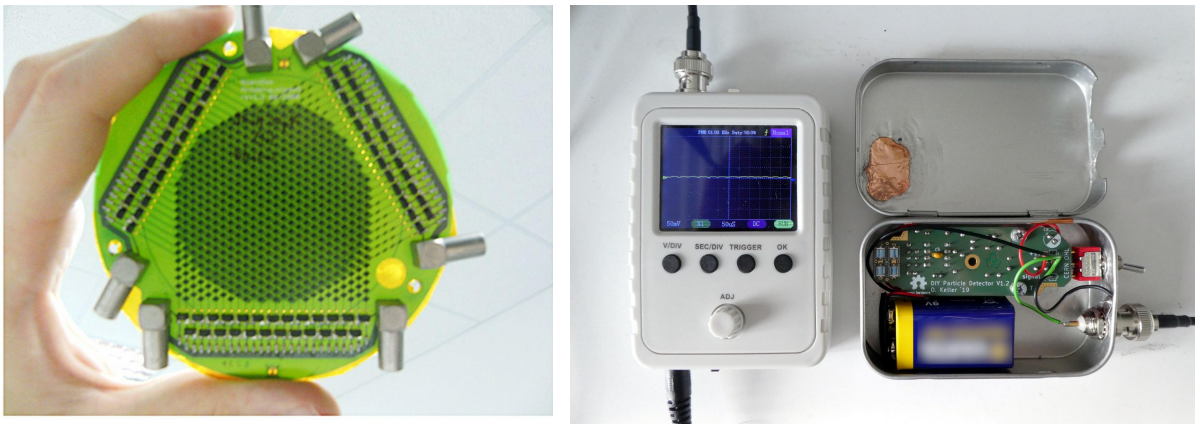


*Fig. 12: Hands-on tutorial experiments provided at the EURIZON detector school. Left: MCP-PMT with delay line anode. Right: do-it-yourself electron spectrometer using low-cost components.*

## 7. Conclusion

One of the primary objectives within the project was to investigate the possibility of reaching a Cherenkov angle resolution of less than 1 mrad. This would be required for the separation of pions and muons up to 3σ in the low-momentum range up to 1.2 GeV/c.

With prototype detectors within this project, both for cosmic muon detection and for pions and protons in CERN test beam experiments, less than 10 mrad have been reached.

In order to reach even better resolutions, sophisticated methods such as dispersion correction have been developed. Other possibilities are limiting the wavelengths by filters in the optical system or anodes only sensitive to a certain wavelength interval.

In addition to the proposed STCF, there are plans for upgrades of other high luminosity e+e– machines. For example a beam polarisation upgrade for Belle II at the SuperKEKB collider is being discussed, with upgraded detectors. For Belle II the momentum range is higher, i.e. up to 4 GeV/c, and a resolution of less than 1 mrad may come within reach.

Concerning the requirements on the technical side, within this project several advances were achieved, in particular for single photon detection and radiation hardness.

This project has received funding from the European Union's Horizon 2020 research and innovation programme under grant agreement No. 871072.

## References

[Sch21] Mustafa Schmidt et al., Status Report on R&D work on particle identification system for the SCT detector, EURIYON Project Deliverable 5.4, full text available at:
https://www.eurizon-project.eu/results/deliverables/

[Bod20] Simon Bodenschatz, Michael Düren, Avetik Hayrapetyan, Ilknur Köseoglu, Marc Strickert, Mustafa Schmidt, The Gießen Cosmic Station - A muon telescope for tests of particle detectors, Journal of Instrumentation 15.C06025 (2020).

[Wel21] Leonard Welde, Optimierung des Trigger-Systems der Giessen Cosmic Station, Bachelor Thesis, 2021

[Kös21] İlknur Köseoğlu-Sarı, Development of a fast readout system for the DISC DIRC prototype of PANDA, Ph. D. Thesis, 2021

[Brü22] Lisa Marie Brück, Bestimmung der Eigenschaften eines DIRC-Prototypen mithilfe rekonstruierter Myonen in der Giessen Cosmic Station, Master Thesis, 2022

[Hof22] Jan Niclas Hofmann, Aufbau und Evaluierung eines Mini-RICH Detektors mit SiPM Sensoren in der Giessen Cosmic Station, Master Thesis, 2022

[Sch17] Mustafa André Schmidt, Particle Identification with the Endcap Disc DIRC for PANDA, Ph. D. Thesis, 2017

[Tak21] Chris Noel Takatsch, Single photon measurements with silicon photomultipliers, Bachelor-Thesis, 2021

[Keg22] Sophie Kegel, Development of compact focusing optics for a Disc DIRC Cherenkov detector, Master Thesis, 2022

[Wet22] Vincent Maximilian Wettig, Monte-Carlo-Simulation of a Disc DIRC Cherenkov Detector with Dispersion Correction, Master Thesis, 2022

[Pap23] Sarah Pappert, Data Analysis and Radiation Hardness of Readout Electronics for a DIRC Detector, Bachelor Thesis, 2023

[Bod24] Simon Bodenschatz, Ph. D. Thesis, ongoing, expected submission in spring 2024

[Per23] Jhonatan Pereira de Lira, Application of Machine Learning Algorithms in the Reconstruction of the Cherenkov Angle in a Disc DIRC detector, Master Thesis, 2023

This project has received funding from the European Union's Horizon 2020 research and innovation programme under grant agreement No. 871072.